An optimization procedure for Microgrid day-ahead operation in the presence of CHP facilities

Published source: http://dx.doi.org/10.1016/j.segan.2017.07.003

An optimization procedure for Microgrid day-ahead operation in the presence of CHP facilities

B. Aluisio[a], M. Dicorato[a], G. Forte[a], M. Trovato[a,*]

[a] DEI – Politecnico di Bari, via E. Orabona 4, 70125, Bari, Italy

Abstract

Microgrids are more and more called to satisfy, through the management of distributed generation sources and the electricity network, the demand for energy by local users. The simultaneous production of electrical and thermal energy by means of Combined Heat and Power (CHP) systems represents one of the features of a Microgrid and can contribute to improve system reliability, efficiency and economic performance. In this paper, an optimization procedure for day-ahead scheduling of a CHP-based Microgrid is developed, aiming to minimize operation and emission costs of Microgrid components in the presence of electric and thermal loads and renewable forecasts. To this purpose, four different operating strategies for CHP are accounted in Microgrid framework. The proposed methodology is based on a non-linear optimization technique and it is applied to the determination of day ahead operation program, with 15-minutes time step, for realistic model of an experimental Microgrid.

Keywords

Microgrid

* Corresponding author.
Mail to: DEI – Politecnico di Bari, via E. Orabona 4, 70125, Bari, Italy
E-mail: micheleantonio.trovato@poliba.it
Ph.: +39 080 5963244
Fax: +39 080 5963410

Published source: http://dx.doi.org/10.1016/j.segan.2017.07.003

Combined Heat and Power

day-ahead scheduling

energy storage

distributed generation

Nomenclature

Indices:

i Micro-Turbine based cogeneration system (MT)

k Reciprocating-Engine based cogeneration system (RE)

j Boiler

s Energy Storage System (ESS)

z Electrical Load

h Thermal Load

g Photovoltaic generator (PV)

r Wind Turbine (WT)

t Time period

Parameters:

n_M Total number of MTs

n_R Total number of REs

n_B Total number of boilers

n_S Total number of ESSs

n_L Total number of electrical loads

n_H Total number of thermal loads

Published source: http://dx.doi.org/10.1016/j.segan.2017.07.003

n_{PV} Total number of PVs

n_{WT} Total number of WTs

N Total number of time periods $(t = 1, 2, ..., N)$

Input Variables:

P_{zt}^{L} Electric power demand of z-th load in the t-th time period

P_{gt}^{V} Electric power generated by g-th PV in the t-th time period

P_{rt}^{W} Electric power generated by r-th WT in the t-th time period

Q_{ht} Demand of h-th thermal load in the t-th time period

State Variables:

P_{it}^{M} Electric power generated by i-th MT in the t-th time period

P_{kt}^{R} Electric power generated by k-th RE in the t-th time period

P_{st}^{C} Charging power of s-th ESS in the t-th time period

P_{st}^{D} Discharging power of s-th ESS in the t-th time period

E_{st} State Of Charge (SOC) of s-th ESS in the t-th time period

P_{Pt} Electric power withdrawn from distribution network at Point of Common Coupling (PCC) in the t-th time period

P_{Dt} Electric power delivered to distribution network at PCC in the t-th time period

Q_{jt}^{B} Thermal power generated by the j-th boiler in the t-th time period

Cost items:

$C(P_{it}^{M})$ operation cost of i-th MT in the t-th time period

Published source: http://dx.doi.org/10.1016/j.segan.2017.07.003

$S(P_{it}^{M})$ emission cost of i-th MT in the t-th time period

$C(P_{kt}^{R})$ operation cost of k-th RE in the t-th time period

$S(P_{kt}^{R})$ operation cost of k-th RE in the t-th time period

$C(Q_{jt}^{B})$ operation cost of j-th boiler in the t-th time period

$S(Q_{jt}^{B})$ emission cost of j-th boiler in the t-th time period

$C\left(P_{Pt}\right)$ cost for electricity purchase at PCC

$R\left(P_{Dt}\right)$ revenue for electricity delivery at PCC

Constants:

$\overline{P}_i^M, \underline{P}_i^M$ Maximum and minimum value of P_{it}^M

$\overline{P}_k^R, \underline{P}_k^R$ Maximum and minimum value of P_{kt}^R

$\overline{Q}_j^B, \underline{Q}_j^B$ Maximum and minimum value of Q_{jt}^B

$\overline{P}_{Pt}, \overline{P}_{Dt}$ Maximum values of P_{Pt} and P_{Dt} at time t

$\overline{P}_s^C, \overline{P}_s^D$ Maximum values of P_{st}^C and P_{st}^D

$\overline{E}_s, \underline{E}_s$ Maximum and minimum value of E_{st}

Δt Amplitude of the t-th time period

1. Introduction

Microgrid (MG) is an ensemble of Distributed Generation (DG) technologies, Energy Storage Systems (ESSs) and electrical and thermal loads which can operate autonomously or in grid-connected mode. DG technologies typically include photovoltaic (PV) and wind turbines (WT), microturbines (MT) and reciprocating internal combustion engines (RE).

The MG concept is based on two typical aspects: it is designed to supply electrical and thermal loads for a small community, operating as a controlled entity connected to the distribution network by the Point of Common Coupling (PCC) [1][2].

In general, the MG is monitored and controlled in real time through a hierarchical control structure including a central controller and local-source controllers. The central controller performs several functions at the highest level, such as energy management, security assessment, state estimation, protection coordination. Local controllers act in a coordinated way, to ensure each component to operate in its rated range and to carry out control strategies developed at central level [2].

In the field of energy management procedures, the optimal scheduling of MG operation is an attractive issue as regards the goal to be pursued (minimum-cost, maximum-profit and/or reliable operation) as well as the current MG configuration (grid-connected or islanded). Day-ahead scheduling is called to determine generation profiles of controllable sources according to forecast demand, whereas real time dispatching involves adjustments in order to smooth out load variation and renewable power fluctuations [3][4].

Different solutions have been proposed to approach the MG energy management problem. A thorough review of relevant methodologies, classified according to objective functions, optimization techniques, solution approaches and exploited software tools is reported in [5].

In [6], several operation strategies are shown, with the purpose of minimizing operation cost using DG sources only for periods in which using batteries is not convenient. In

Published source: http://dx.doi.org/10.1016/j.segan.2017.07.003

[7], two strategies for the optimal management of ESS in a MG are proposed. An economic benefit maximization problem is considered in [8], where minimum on-off time constraints and ramping constraints are taken into account. In [9], user costs for Load Shedding are considered using PowerWorld Simulator®. A strategy for managing a MG containing PVs and hybrid ESSs is proposed in [10]. Whereas, an operation planning of MG considering time-of-use pricing is developed in [11], allowing to program the MG operation on the basis of electricity price trend. In [12], a multi-objective function is considered for environmental and economic optimization problem, in which pollutant emissions are taken into account through an equivalent cost. In [13], a multi-objective optimization integrated with network reconfiguration problem is executed. In [14], both day-ahead operational scheduling and unit commitment problems are considered in the presence of controllable loads. In [15], several objectives for microgrid optimal operation programming are weighed in a single function in order to prove the effectiveness of weighing coefficients.

Another crucial aspect in MG operation programming is the prediction of generated power from renewable sources. To this purpose, several methods based on Neural Networks are proposed in [16]. A stochastic approach is used in [17], to take into account prediction uncertainty in MG operation programming. Robust optimization is accounted in [18] to account for reserve needs to deal with possible deviations of wind generation from forecast levels, whereas load uncertainty and reliability costs are added in robust optimization in [19].

Recently, optimization of MG operation considering both electric and thermal demands has become of primary importance. In particular, the use of Combined Heat and Power (CHP) systems enforces the interactions among different energy forms and improve the

Published source: http://dx.doi.org/10.1016/j.segan.2017.07.003

efficiency of energy supply in a MG [20]. For instance, in [21] CHP modelling is accounted along with an operating strategy of thermal storage in order to determine hourly MG plan. An advanced model of CHP, including cooling demand and involving ambient influence, is developed in [4]. The influence of heat pumps in the satisfaction of electric and thermal demand of a domestic MG is tackled in [22]. In [23] the optimal dispatch of microgrid with CHP is based on probabilistic algorithm accounting for load and renewable probability distribution function and with linear CHP costs, whereas in [24] the daily scheduling of CHP-based MG is based on a stochastic model involving CHP cost as quadratic function of electric and heat power production and considering feasible operating region linking electric and heat output typical of combined-cycle plants. Moreover, in [25] economic emission load dispatch scheduling in a MG with CHPs is based on quadratic cost function and the determination of emission merit order according to Differential Evolution Technique. In [26] linear formulation of the production cost function is provided in combination with the coordination cost to cover both heat and power demands. A linear problem of optimal scheduling of a CHP system in thermal following mode with energy storage is depicted in [27]. The influence of different charge schemes of electricity purchase on operation planning of energy smart homes including CHP is depicted in [28].

The aim of this work is to propose a procedure for optimal day-ahead operation scheduling of a MG, which is one of the tasks performed by MG Central Controller. A particular focus is devoted to proper modelling of CHP operation suitable for microgrid size and their integration with back-up boilers, in order to cover electric and thermal demand. A detailed characterization of MG components and electric/thermal load is provided, along with relevant suitable constraints, and differentiated costs for power exchange from/to the distribution network at PCC are considered. The presence of several thermal loads in the same MG not connected to each other but sharing the electric production is considered as well. In addition, different operation strategies for CHP-based generators are embedded in the procedure, in order to prove the effectiveness of electric and thermal demand coverage assumptions. A non-linear formulation of day-ahead scheduling problem is provided and the procedure is implemented in MatLab adopting SQP solver. The proposed methodology is tailored to be implemented in a SCADA/EMS system of an experimental MG, and the paper presents the results of program development, planning to be implemented in a real MG facility. As compared to the approaches in literature dealing with the operation planning of CHP-based MG, the novel contributions of the paper are:

i) the characterization of typical operating modalities of CHP systems, as described in [29] and [30] for autonomous systems, in MG operation planning framework. These strategies are usually neglected in other formulations or only one of them is assumed [27][31];

ii) the adoption of realistic nonlinear efficiency functions for CHPs, instead of constant values as in [20][28][32][33];

iii) the integration in a single MG, sharing all electric production facilities, of several sources for the coverage of distinct thermal loads instead of considering a single aggregate thermal demand. Moreover, the presence of excess heat ensures higher flexibility [25][34];

iv) the analysis on day-ahead horizon with 15-min programming time step, more and more necessary to capture variations of renewable production [35], assuming the

Published source: http://dx.doi.org/10.1016/j.segan.2017.07.003

presence of a second control stage, closer to real time operation, to deal with deviations from forecast values [36];

v) the exploitation of SQP method for the solution of the complete nonlinear optimization problem instead of mixed-integer linear programming that can lose information [37] or mixed-integer nonlinear programming that could not reach feasible point [38];

vi) the test of real CHP system operation integrated in an experimental MG.

The paper is organized as follows. In Section II, mathematical representation of MG components is proposed. Section III deals with MG day-ahead scheduling problem, and in Section IV test case and results are presented.

2. Modeling of Microgrid components

Exploitable technologies in a MG can be divided into different groups. Technologies based on non-programmable renewable energy sources (RES), such as wind speed, solar radiation and water flow, produce energy without significant control, therefore their contribution should be at most forecasted but could be affected by remarkable variations. An ESS can influence the operation of the MG by performing several tasks, such as improve the reliability and mitigate the uncertainty of electricity production by RESs. MTs and REs generate electrical power and useable exhaust heat which can provide hot water or process heat, and can run on a variety of fuels, allowing flexibility in the case of fuel unavailability and volatile fuel prices. Moreover, boilers usually compensate the action of CHP systems to cover thermal demand variations.

In this Section, models of MG components for the representation of economic and operation features in a day-ahead time interval are described. To this purpose, energy

Published source: http://dx.doi.org/10.1016/j.segan.2017.07.003

production facilities based on non-programmable renewable energy sources have generally negligible operation costs, since no buying cost is associated to the source, whereas their production level in each interval of the day-ahead horizon is linked to expected value of the forecast of source availability. Moreover, since they take part to the MG that is a single entity interfacing the distribution network and eventually the market, nor economic penalizations are ascribable to forecast errors neither specific incentive schemes are accounted. On the other hand, programmable energy production devices (e.g. fuel-based generation apparatus, as well as external network) can be fully controlled but incur in remarkable short-term operation costs. Energy storage devices, similarly to RES-based systems, have generally no variable cost, but are subject to internal state variation and conversion losses.

The proposed distinction is reflected in the following formulation of device models for day-ahead operation planning. In fact, WT and PV power production is linked to ambient condition forecasts and no variable cost is accounted, whereas variable costs are considered for MT, RE, boilers and grid connection. Storage devices involve loss terms with no variable cost.

2.1. Wind turbine

The power output of the *r*-th WT in the *t*-th time interval, according to a given value of wind speed v_{rt}, depending on ground clearance and roughness, is evaluated as follows:

$$P_{rt}^{W} = \begin{cases} f(v_{rt}) & \underline{v}_r \le v_{rt} \le \tilde{v}_r \\ \tilde{P}_r^{W} & \tilde{v}_r \le v_{rt} \le \overline{v}_r \\ 0 & else \end{cases} \tag{1}$$

where $\tilde{P}_r^W$ is the rated power of the WT, $\underline{v}_r$, $\tilde{v}_r$, $\overline{v}_r$ are the cut-in, rated and cut-off wind speed, respectively, and $f(v_{rt})$ is a polynomial function representing power-speed curve of the WT. Suitable forecasting procedure or historical data can be exploited to obtain v_{rt} over a time interval [39].

2.2. Photovoltaic generator

The output power of the *g*-th PV generator at the *t*-th time interval is expressed as follows:

$$P_{gt}^V = \gamma_g \cdot n_g^V \cdot \zeta_g^V(\theta_{gt}) \cdot A_g \cdot I_{gt} \tag{2}$$

where I_{gt} [kW/m^2] is the incident irradiance on panel surface, taking into account direct, diffuse and reflected components [40], A_g [m^2] is the panel area, n_g^V is the number of panels in the PV system, $\zeta_g^V(\theta_{gt})$ is panel efficiency depending on its temperature θ_{gt} [41], and γ_g is a degradation coefficient accounting for shading, inverter and asymmetries losses. Solar irradiance can be estimated according to forecast procedures or historical data [42].

2.3. Energy storage system

The operation of an ESS is characterized by its energy content, or State Of Charge (SOC). The SOC of the *s*-th ESS in *t*-th time stage is related to capacity left at previous stage t_- , as follows:

$$E_{st} = (1 - q_s^D) \cdot E_{st_-} + \left(P_{st}^C \cdot \Delta t \cdot \psi_s^C\left(P_{st}^C\right)\right) - \left(\frac{P_{st}^D \cdot \Delta t}{\psi_s^D\left(P_{st}^D\right)} \right) \tag{3.a}$$

where $\psi_s^C\left(P_{st}^C\right)$ and $\psi_s^D\left(P_{st}^D\right)$ are the charging and the discharging efficiency of the *s*-

Published source: http://dx.doi.org/10.1016/j.segan.2017.07.003

th ESS, respectively, depending on charge and discharge power level, and the self-discharging effect is accounted by means of a quota q_s^D of available capacity at previous stage [43][44]. At the first time step, $t = 1$, it is assumed that $t\_ = N$ so that the same state is present at the extremes of the day. Moreover, the following relation holds, in order to fix the SOC at the beginning of programming horizon to a value $E_s^{'}$ able to guarantee an efficient daily operation in any condition.

$$E_{sN} = E_s^{'} \tag{3.b}$$

The values of SOC and charge/discharge power are limited by technical features and defined operating conditions of the ESS, as follows:

$$\underline{E}_s \le E_{st} \le \overline{E}_s \tag{4.a}$$

$$0 \le P_{st}^C \le \overline{P}_s^C \tag{4.b}$$

$$0 \le P_{st}^D \le \overline{P}_s^D \tag{4.c}$$

In particular, maximum SOC value in equation (4.a) is determined as $\overline{E}_s = \mu_s \cdot E_s^{nom}$ where E_s^{nom} is the nameplate energy capacity of the ESS and μ_s represents the capacity reduction factor. This factor depends on the utilization history of the ESS, i.e. equivalent cycles at the defined depth of discharge [45][46][47], from the beginning of exploitation, and it is updated for the analysis of different days.

Moreover, for each time interval, it is assumed that the ESS could only be charged or discharged. Therefore, the following condition holds:

$$P_{st}^C \cdot P_{st}^D = 0 \tag{4.d}$$

2.4. MicroTurbine based Cogeneration System

Published source: http://dx.doi.org/10.1016/j.segan.2017.07.003

The operation cost of *i*-th MT can be evaluated as follows [48]:

$$C(P_{it}^{M}) = \varphi_i^M \cdot \frac{\Delta t \cdot P_{it}^{M}}{H_i^M \cdot \eta_i(P_{it}^{M})} \tag{5}$$

where φ_i^M [€ per fuel unit] is the cost of fuel (generally natural gas), H_i^M [kWh per fuel unit] is the lower heating value of fuel and $\eta_i(P_{it}^M)$ is the electrical efficiency at specific level of power production P_{it}^M . The latter has to be within technical limits of the MT:

$$\underline{P}_i^M \le P_{it}^M \le \overline{P}_i^M \tag{6}$$

Whenever the *i*-th MT operates in CHP mode, its exploitable thermal output in the *t*-th time stage Q_{it}^M can be obtained by the following expression [49]:

$$Q_{it}^M = P_{it}^M \cdot \frac{\xi_i^M}{\eta_i(P_{it}^M)} \tag{7}$$

where ξ_i^M represents the thermal efficiency.

In order to determine a proper tradeoff between fuel expenses and pollutant emissions, the equivalent cost of CO_2 emissions is employed, by means of a unit penalty cost σ_E [€/kg]. The equivalent emission cost of the *i*-th MT can be evaluated as follows:

$$S(P_{it}^M) = \sigma_E \cdot \varepsilon_i(P_{it}^M) \cdot \Delta t \cdot P_{it}^M \tag{8}$$

where $\varepsilon_i(P_{it}^M)$ [kg/kWh] is the emission factor of the *i*-th MT, determined as $\varepsilon_i(P_{it}^M) = \overline{\varepsilon}_i^M / \eta_i(P_{it}^M)$, being $\overline{\varepsilon}_i^M$ a constant emission factor depending on the burnt fuel in the *i*-th MT.

Moreover, ramping limits can be neglected in the day-ahead horizon with reasonably wide time step [4].

2.5. Reciprocating-Engine based Cogeneration System

The operation cost of *k*-th RE system in the *t*-th time stage can have the following expression [50]:

$$C(P_{kt}^{R}) = \varphi_k^R \cdot \frac{\Delta t \cdot P_{kt}^{R}}{H_k^R \cdot \eta_k(P_{kt}^{R})} \tag{9}$$

where φ_k^R [€ per fuel unit] is the fuel cost, H_k^R [kWh per fuel unit] is the lower heating value of fuel, $\eta_k(P_{kt}^{R})$ is the electrical efficiency. Power production of the RE P_{kt}^{R} is limited by technical features:

$$\underline{P}_k^R \le P_{kt}^{R} \le \overline{P}_k^R \tag{10}$$

Moreover, in CHP mode, the useable thermal power from *k*-th RE system at the *t*-th time interval Q_{kt}^{R} can be evaluated as follows [49]:

$$Q_{kt}^{R} = P_{kt}^{R} \cdot \frac{\xi_k^R}{\eta_k(P_{kt}^{R})} \tag{11}$$

where ξ_k^R is the thermal efficiency.

The equivalent cost of CO_2 emissions can be calculated as:

$$S(P_{kt}^{R}) = \sigma_E \cdot \varepsilon_k(P_{kt}^{R}) \cdot \Delta t \cdot P_{kt}^{R} \tag{12}$$

where $\varepsilon_k(P_{kt}^{R})$ [kg/kWh] is the emission factor of the *k*-th RE, determined as $\varepsilon_k(P_{kt}^{R}) = \overline{\varepsilon}_k^R / \eta_k(P_{kt}^{R})$, being $\overline{\varepsilon}_k^R$ a constant emission factor depending on the burnt fuel in the *k*-th RE.

Published source: http://dx.doi.org/10.1016/j.segan.2017.07.003

2.6. Boiler

The operation cost of the *j*-th boiler in the *t*-th time stage can be expressed as [51]:

$$C(Q_{jt}^{B}) = \varphi_{j}^{B} \cdot \frac{\Delta t \cdot Q_{jt}^{B}}{H_{j}^{B} \cdot \xi_{j}^{B}} \tag{13}$$

where φ_{j}^{B} is the fuel cost [€ per fuel unit], H_{j}^{B} [kWh per fuel unit] is the lower heating value, ξ_{j}^{B} is the thermal efficiency. The thermal power produced by the *j*-th boiler Q_{jt}^{B} is limited in the range:

$$\underline{Q}_{j}^{B} \le Q_{jt}^{B} \le \overline{Q}_{j}^{B} \tag{14}$$

The equivalent cost of CO_2 emissions from the *j*-th boiler can be evaluated by the expression:

$$S(Q_{jt}^{B}) = \sigma_{E} \cdot \varepsilon_{j}(Q_{jt}^{B}) \cdot \Delta t \cdot Q_{jt}^{B} \tag{15}$$

where $\varepsilon_{j}(Q_{jt}^{B})$ [kg/kWh] is the emission factor of the *j*-th boiler referred to thermal power production.

2.7. Power exchange at PCC

In the grid-connected mode, the cost of electric energy withdrawal at PCC from the distribution network in the *t*-th time step is given by the expression:

$$C\left(P_{Pt}\right) = \pi_{Pt} \cdot \Delta t \cdot P_{Pt} \tag{16}$$

where π_{Pt} [€/kWh] is the electricity purchase price, and P_{Pt} is limited by a constraint deriving from contractual conditions of energy purchase:

$$0 \ge P_{Pt} \ge \overline{P}_{Pt} \tag{17}$$

Whereas, the revenue from the energy delivered at PCC to the distribution network can

Published source: http://dx.doi.org/10.1016/j.segan.2017.07.003

be put in the form:

$$R\left(P_{Dt}\right) = k_D \cdot \pi_{Dt} \cdot \Delta t \cdot P_{Dt} \tag{18}$$

where π_{Dt} is the electricity selling price, $k_D < 1$ is a coefficient that takes into account the economic burden of connection service [52]. Analogously to power purchase, the delivered amount P_{Dt} has to be below a contractual fixed value:

$$0 \geq P_{Dt} \geq \overline{P}_{Dt} \tag{19}$$

In order to avoid bidirectional power exchange at PCC in a single *t*-th time interval, the following condition holds:

$$P_{Pt} \cdot P_{Dt} = 0 \tag{20}$$

3. Day-ahead energy management problem

In this Section, a nonlinear optimization procedure is formulated for the day-ahead scheduling of the MG generation sources in order to meet the internal electric and thermal demand by minimizing operation costs and environmental impacts.

3.1. Problem formulation

The MG energy management function is performed through the solution of a non-linear optimization problem, aiming to minimize an objective function subject to equality and inequality constraints, that can be posed in the following canonical form:

$$\begin{gathered} \min_{\boldsymbol{x}} \; J\left(\boldsymbol{x}\right) \\ \text{subject to} \begin{cases} \boldsymbol{g}(\boldsymbol{x}) = \boldsymbol{0} \\ \boldsymbol{h}(\boldsymbol{x}) \leq \boldsymbol{0} \end{cases} \end{gathered} \tag{21}$$

where $\boldsymbol{x}$ is a $\left(n_M + n_R + n_B + 3 \cdot n_S + 2\right) \cdot N$ dimensional vector including the subsets of

Published source: http://dx.doi.org/10.1016/j.segan.2017.07.003

variables $\left\{P_{it}^{M}\right\},\left\{P_{kt}^{R}\right\},\left\{Q_{jt}^{B}\right\},\left\{P_{st}^{C}\right\},\left\{P_{st}^{D}\right\},\left\{E_{st}\right\},\left\{P_{Pt}\right\},\left\{P_{Dt}\right\}$ and $J\left(\boldsymbol{x}\right)$ includes the MG operation and emission costs over the total time interval $N\cdot\Delta t$, expressed as follows:

$$J\left(\boldsymbol{x}\right)=\sum_{t=1}^{N}\left\{C(P_{Pt})-R(P_{Dt})+\sum_{i=1}^{n_M}\left[C(P_{it}^{M})+S(P_{it}^{M})\right]+\right. \\ \left.+\sum_{k=1}^{n_R}\left[C(P_{kt}^{R})+S(P_{kt}^{R})\right]+\sum_{j=1}^{n_B}\left[C(Q_{jt}^{B})+S(Q_{jt}^{B})\right]\right\} \tag{22}$$

Equality constraints in (21) include the subsets: (3.a), giving out $n_S\cdot N$ linear relations for all storage devices in the whole time horizon; (3.b), with n_S linear equations; (4.d), constituting $n_S\cdot N$ non-linear conditions; (20), corresponding to N non-linear constraints. Moreover, the electrical power balance of the MG in the *t*-th time period is imposed, requiring that the sum of load demand of all electricity users taking part to the MG and net power interchange with the distribution network equals the production of internal energy sources, neglecting MG losses in the day-ahead programming stage, as follows:

$$\sum_{z=1}^{n_L}P_{zt}^{L}+(P_{Dt}-P_{Pt})=\sum_{i=1}^{n_M}P_{it}^{M}+\sum_{k=1}^{n_R}P_{kt}^{R}+\sum_{s=1}^{n_S}(P_{st}^{D}-P_{st}^{C})+\sum_{g=1}^{n_{PV}}P_{gt}^{V}+\sum_{r=1}^{n_{WT}}P_{rt}^{W} \tag{23}$$

By considering that the electricity balance over all the planning horizon involves N linear constraints, the set of equality constraints $\boldsymbol{g}(\boldsymbol{x})=\boldsymbol{0}$ includes $\left(2\cdot n_S+2\right)\cdot N+n_S$ relations.

Furthermore, inequality constraints in (21) are represented by the subsets: (4.a)-(4.c), constituting $6\cdot n_S\cdot N$ linear conditions; (6), involving $2\cdot n_M\cdot N$ linear relations; (10),

Published source: http://dx.doi.org/10.1016/j.segan.2017.07.003

yielding $2 \cdot n_R \cdot N$ linear constraints; (14), constituting $2 \cdot n_B \cdot N$ linear inequalities; (17) and (19), giving rise to $2 \cdot N$ linear relations each. Moreover, thermal power balance is dealt with, accounting for the technologies involved in thermal energy production, i.e. CHP units and Boilers. In accordance with the operation criteria of the MG, the possibility that a part of thermal energy can be released to the atmosphere at a given time period is considered. In particular, it is supposed that a part of the exhaust air after combustion, controlled by means of valves, passes through the exchangers to give useful heat, and a ventilation system, whose electric demand can be considered negligible, lets exhausts leave the thermal supply. In addition, the presence of different thermal loads, i.e. groups of users served by a determined subset of thermal power sources in the MG framework, is accounted. The link between the *h*-th thermal load and the thermal power sources of MG at the *t*-th time period can be expressed by the following inequality:

$$Q_{ht} \le \sum_{i=1}^{n_M} a_{hi}^M \cdot Q_{it}^M + \sum_{k=1}^{n_R} a_{hk}^R \cdot Q_{kt}^R + \sum_{j=1}^{n_B} a_{hj}^B \cdot Q_{jt}^B \tag{24}$$

where Q_{it}^M and Q_{kt}^R are evaluated by the non-linear expressions (7) and (11), respectively. Moreover, the coefficients a_{hi}^M, a_{hk}^R and a_{hj}^B are equal to 1 if the correspondent *i*-th MT, *k*-th RE or *j*-th boiler, respectively, is connected to the *h*-th thermal load, otherwise they are equal to zero.

Since the thermal power balance for all thermal users over the planning horizon involves $n_H \cdot N$ non-linear relations, the size of inequality constraint set $\boldsymbol{h}(\boldsymbol{x}) \le \boldsymbol{0}$ is $(2 \cdot n_M + 2 \cdot n_R + 2 \cdot n_B + 6 \cdot n_S + n_H + 4) \cdot N$.

The described methodology has the advantage to include a wide set of the technologies taking part to a MG, and slight variations can allow to model other specific devices. The adopted models allow to catch the behaviour of MG-sized devices in the day-ahead horizon, where the ramping limits can be neglected and steady-state conditions can be considered valid for each time step. Moreover, it is worth to remark that the procedure is able to simulate the islanded mode condition of MG operation in defined time steps, by assuming $\overline{P}_{Pt} = 0$ and $\overline{P}_{Dt} = 0$. This implies that grid costs do not affect the objective function in that specific time period and the electricity balance cannot rely on flexibility ensured by distribution network exchange. Hence, the optimal day-ahead operation plan is determined on the basis of the sole MG internal sources.

3.2. CHP Operation Strategies

The solution of problem (21) provides the optimal values of the outputs of CHP devices, boilers and ESS, on the basis of expected contributions by PV and WT systems, to satisfy the load demand.

However, ad hoc strategies for managing CHP units can be required to improve long-term technology performance and to comply with specific needs [30]:

- C1. *electrical load tracking*: selected CHP units are managed with the aim of following the evolution of electricity load;
- C2. *thermal load tracking*: specified CHP units are operated with the objective of following the behavior of defined heating loads;
- C3. *on-off operation:* given CHP units are operated at the rated output over defined time periods.

The C1 strategy can be easily handled, by adding to the problem (21), for each time

Published source: http://dx.doi.org/10.1016/j.segan.2017.07.003

stage, the following equality constraint:

$$\alpha_t \cdot \sum_{z=1}^{n_L} P_{zt}^L = \left[\sum_{i=1}^{n_M} b_{it}^M \cdot P_{it}^M + \sum_{k=1}^{n_R} b_{kt}^R \cdot P_{kt}^R \right] \cdot \beta_t \qquad (25)$$

where the coefficient α_t $\left(0 \le \alpha_t \le 1\right)$ represents the portion of electrical load that is covered at the *t*-th stage by the *i*-th MT or the *k*-th RE, selected by imposing the binary factors b_{it}^M and b_{kt}^R, respectively, equal to 1. At the *t*-th time step, the C1 strategy is activated by $\beta_t = 1$ and $\alpha_t \ne 0$, whereas, as long as $\beta_t = 0$, $\alpha_t = 0$ and C1 strategy is not applied. Therefore, the activation of C1 strategy yields the increase of equality constraints to a total of $\left(2 \cdot n_S + 3\right) \cdot N + n_S$ relations.

The C2 strategy is modeled by introducing, for the *h*-th thermal load and for the *t*-th time step, the following equality condition:

$$\alpha_{ht} \cdot Q_{ht} = \left[\sum_{i=1}^{n_M} u_{it}^M \cdot a_{hi}^M \cdot Q_{it}^M + \sum_{k=1}^{n_R} u_{kt}^R \cdot a_{hk}^R \cdot Q_{kt}^R \right] \cdot \beta_{ht} \qquad (26)$$

where the coefficient α_{ht} $\left(0 \le \alpha_{ht} \le 1\right)$ represents the portion of *h*-th thermal load that is fed at the *t*-th step by the *i*-th MT or the *k*-th RE selected by imposing the binary factors u_{it}^M and u_{kt}^R, respectively, equal to 1. At the *t*-th time step and for the *h*-th thermal load, the C2 strategy is in force if $\beta_{ht} = 1$ and $\alpha_{ht} \ne 0$, whereas, as long as $\beta_{ht} = 0$, $\alpha_{ht} = 0$ and C2 strategy is not applied. Therefore, the presence of C2 strategy involves a total of $\left(2 \cdot n_S + 2 + n_H\right) \cdot N + n_S$ equality constraints.

The C3 strategy can be implemented by introducing, for the *i*-th MT and/or the *k*-th RE, the following relations:

Published source: http://dx.doi.org/10.1016/j.segan.2017.07.003

$$\beta_{it}^{M} \cdot P_{it}^{M} = \beta_{it}^{M} \cdot \overline{P}_{it}^{M} \tag{27.a}$$

$$\beta_{kt}^{R} \cdot P_{kt}^{R} = \beta_{kt}^{R} \cdot \overline{P}_{kt}^{R} \tag{27.b}$$

The strategy is activated, for the *i*-th MT or the *k*-th RE, if for the *t*-th time step, the binary factors β_{it}^{M} or β_{kt}^{R} is equal to 1, respectively. Whereas, as long as $\beta_{it}^{M}=0$ or $\beta_{kt}^{R}=0$, the C3 strategy is not applied. Therefore, the presence of C3 strategy involves a total of $\left(2 \cdot n_S + 2 + n_M + n_R\right) \cdot N + n_S$ equality constraints.

4. Test Results

4.1. The test MG under study

The proposed optimization procedure and CHP strategies are applied to the test MG shown in Fig. 1.

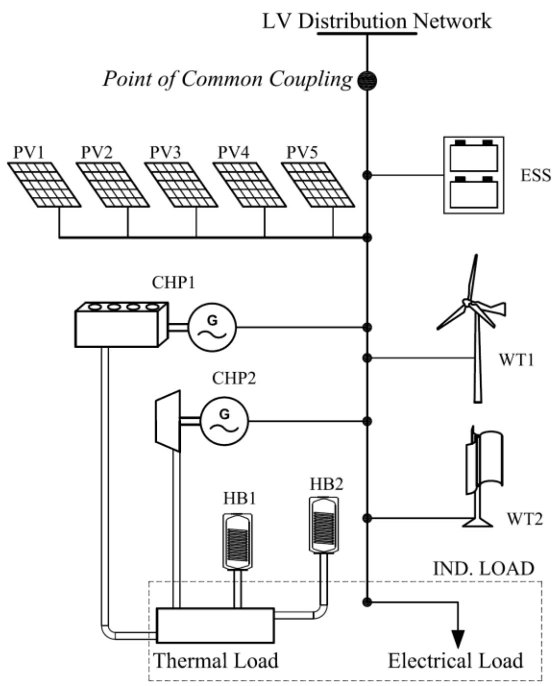

Fig. 1. The test MG.

The test MG represents a selected configuration of experimental facility built at Power and Energy System laboratory of Politecnico di Bari thanks to EU funds [53] with improved thermal section, currently under integration. The experimental facility is a low-voltage network, that can be operated in grid-connected or islanded mode, including the following devices:

- a gas-fueled CHP system, equipped with two variable-speed REs with total 105 kW rated electric power;
- a gas MT with 30 kW nominal power;
- a 50-kW photovoltaic field composed of five sub-arrays with different panel technologies;
- a sodium-nickel battery working at roughly 260 °C, with a discharge duration of 3 hours;
- a 60-kVA wind turbine emulator, based on a back-to-back converter controlled according to models of different mini-wind generators and to measurement of an anemometer;
- two programmable loads, with 150 kVA rated power each, able to replicate active and reactive power needs of different kinds of load;
- a by-pass converter, with 200 kVA rated power, which allows the power exchange with the main network to be fixed at a specified value.

The facility is equipped with a Modbus/TCP-IP communication network, and it is monitored and controlled by means of a proper SCADA/EMS system, based on a hierarchical structure [54]. The proposed day-ahead operation planning function is aimed to be implemented in the SCADA system by means of software integration ensured by Open Platform Communication (OPC) environment. Therefore, the proposed procedure is currently object of real-world implementation.

The main characteristics of test MG components for the relations described in Section 2 are described in Table 1 for renewable-based components and in Table 2 for other devices. For the employed ESS, available depth of discharge is 80%, self-discharging effect is assumed negligible in the daily time horizon, charge and discharge efficiencies are observed to be quite independent on power levels, and no previous exploitation is assumed, therefore ESS maximum SOC is equal to rated capacity. The amount of power exchange at PCC is capped at 200 kW on both withdrawal and delivery.

Table 1. Characteristics of renewable devices in the Test MG

Device Name	Description	Rated electric power [kW]	Cut-in / Nominal / Cut-off wind speed [m/s]	PV panel power [W] / module number / nominal efficiency [%]
WT1	33-kW horizontal axis wind turbine	33	3.5 / 11 / 20	
WT2	two 6-kW vertical axis wind turbines	12	5 / 14 / 25	
PV1	photovoltaic triple junction a-Si modules	9.216		144 / 64 / 7.7
PV2	photovoltaic mono-crystalline Si modules	10.53		270 / 39 / 16.6
PV3	photovoltaic poly-crystalline Si modules	10.5		250 / 42 / 15.4
PV3	photovoltaic CIS technology	9.6		150 / 64 / 12.2
PV3	photovoltaic mono N-type modules	9.9		300 / 33 / 18.3

Table 2. Characteristics of non-renewable devices in the Test MG

Device Name	Description	Rated electric (charge/discharge) power [kW]	Rated thermal power [kW]	Rated capacity [kWh]	Rated electric (charge/discharge) efficiency	Rated thermal efficiency
ESS	sodium-nickel chloride battery system	44 / 48	---	141	85% / 85%	---
CHP1	gas-fuelled RE in cogeneration mode	105	180	---	31.5% (Fig. 2)	50%
CHP2	gas MT in cogeneration mode	28	57	---	24.8% (Fig. 2)	50%
B1	wood-fuelled boiler		20			82.5%
B2	pellet-fuelled boiler		75			88.2%

Published source: http://dx.doi.org/10.1016/j.segan.2017.07.003

The electric efficiency trends of CHP systems according to power production level are expressed by means of the following third-order polynomial equations and their trends are depicted in Fig. 2 according to power output in p.u. of nominal power:

$$CHP1:\ \eta_k(P_{kt}^R) = 2.21e-7\cdot(P_{kt}^R)^3 - 7.47e-5\cdot(P_{kt}^R)^2 + 8.06e-3\cdot(P_{kt}^R) + 3.707e-2 \quad (28.a)$$

$$CHP2:\ \eta_i(P_{it}^M) = 2.22e-6\cdot(P_{it}^M)^3 - 3e-4\cdot(P_{it}^M)^2 + 1.397e-2\cdot(P_{it}^M) + 3.905e-2 \quad (28.b)$$

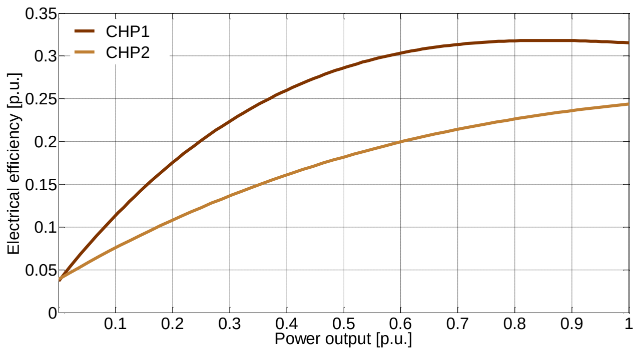

Fig. 2. Electric efficiency trends of CHP systems in the test MG.

Thermal efficiency has been considered constant to the rated values reported in Table 2 both for CHP and boilers, since no remarkable variations are observed during operation. Emission factor for gas burning in CHP1 and CHP2 involves $\bar{\varepsilon}_k^R = \bar{\varepsilon}_i^M = 0.1404\ \mathrm{kg/kWh_{pr}}$ obtaining, at nominal power, 0.453 kg/kWh for CHP1 and 0.560 kg/kWh for CHP2, according to the nameplate data. Whereas, emission factor for boilers is constant, though suitably low (0.002 kg/kWh) due to the exploitation of renewable fuels, whose burning is not related to proper emissions.

Moreover, for each CHP, the minimum production level is set to zero, compatibly to the observed low minimum stable production (roughly 1 kW). Daily curves of electrical and thermal load demand are taken from data of industrial users by an Italian distribution company. Weather data for the forecast of renewable sources production are taken from meteorological stations placed in the considered location [55]. Electric energy purchasing price is determined as the sum of market prices and service costs according to Italian rules, whereas electric energy selling price is defined by the Italian energy authority [52]. Finally, fuel costs are constant and derive from data by a fuel distribution company [56] and are equal to 0.51 €/m^3 for gas, 0.17 €/kg for wood, 0.32 €/kg for pellet, and emission cost is equal to 5.7 €/t [57].

The proposed non-linear optimization methodology is implemented, dividing the day into N = 96 time steps of 15 minutes each, in MatLab® environment and solved through *fmincon* function in Optimization Toolbox exploiting SQP method [58], that has been proved robust for the solution of nonlinear optimization problems, even in non-convex formulations, and it is characterized by superlinear convergence [59][60]. The SQP method is based on the formulation, for each major iteration, of a Quadratic Programming subproblem based on a quadratic approximation of the Lagrangian function with positive semidefinite Hessian matrix and linearized constraints, whose solution is used to form a search direction for a line search procedure with step length according to a merit function [61][62]. As a nonlinear programming method, SQP efficiently looks for a local solution, and the solution search is improved starting from a feasible initial point [62]. In the proposed procedure the initial point is obtained by solving a linearized version of the problem, as suggested in [63]. The linearized problem is built by assuming efficiencies at rated levels, irrespective of power amount, in (3.a), (5), (7), (8), (9), (11), (12), and neglecting nonlinear constraints (4.d) and (20) on bidirectional power flow.

4.2. Test Cases

Simulations are carried out according to data of a typical summer working day, where forecast electricity load amounts to 3,422 kWh in the whole day with a power peak of 165 kW at hour 18. A quota of 14.4% of daily load is covered by forecast RES production, with a peak of 60 kW at hour 12. Moreover, a single thermal load is accounted, analogously to the situation of the experimental facility. It amounts to 4,329 kWh with a maximum of 215 kW at hour 18. ESS initial SOC is set to 0.80 p.u. of rated capacity. Trends of electricity price for the day under investigation are shown in Fig. 3. It is worth to remark that purchasing price varies on hourly basis according to market influence, whereas selling price assumes only 3 different values in the day.

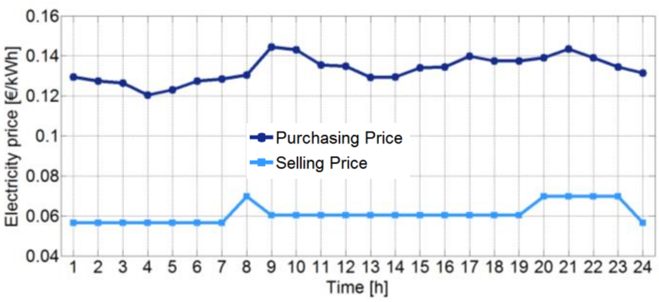

Fig. 3. Electricity price.

Simulations are carried out by applying each CHP strategy described in Section 3.2, and relevant results are compared to the reference solution of the problem reported in Section 3.1 (Base Case).

4.2.1. Base Case

The diagrams of electric power balance and thermal power balance for the Base Case are shown in Figs. 4 and 5, respectively. It can be pointed out that, for the considered day, 75.0% of the daily electric load is satisfied by CHP systems, 8.0% by electricity exchange at PCC, and the share of ESS is 2.8% and is concentrated in early morning and in peak price period in the evening. The sum of these contributions and RES-based

Published source: http://dx.doi.org/10.1016/j.segan.2017.07.003

production (14.4%, as previously stated) exceeds the total daily load, since the supplemental share (3.8%) relates to the charging of the ESS in central hours of the day, and this is ascribable to the compliance with the constraint (3.b). This yields an increase of total MG electricity demand (sum of electric load and ESS charge power), shown in red dashed line in Fig. 4.

The coverage of thermal load is mainly performed by CHPs, with 83.6% contribution of RE (CHP1) and 12.9% by MT (CHP2). These systems work in a different manner, since CHP1 behaves according to load variations, whereas CHP2 is off in early morning and evening, and in central hours of the day it runs at maximum power output. Moreover, B1 helps covering morning peak, contributing by 3.2% to cover thermal load demand, whereas 0.3% of load is covered by B2 in central hours of the day, before CHP2 is on.

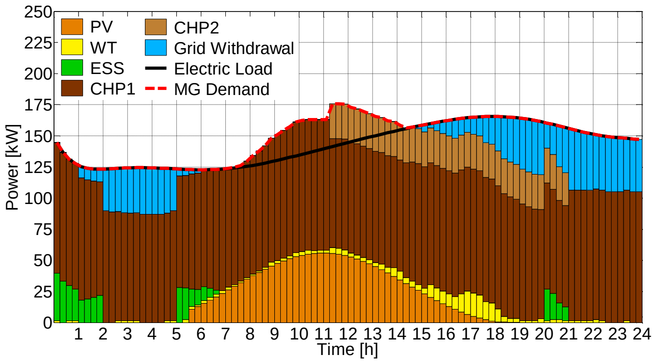

Fig. 4. Base Case Strategy: electrical power balance.

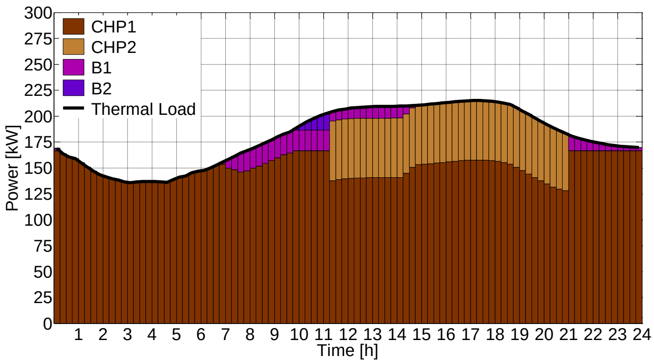

Fig. 5. Base Case Strategy: thermal power balance.

4.2.2. Electrical Load Tracking – C1 Strategy

In order to prove the C1 strategy proposed in Section 3.2, eq. (25) is considered in equality constraints, assuming $\alpha_t = 0.8$ and involving both CHP systems over the whole day ($b_{it}^{M} = 1$ and $b_{kt}^{R} = 1 \ \forall t$). Complying with this requirement, the sum of CHP contributions covers the 80% of electric load profile for each time step of the considered day, as can be noted in Fig. 6. CHP1 and CHP2 cover 69.0% and 11.0% of load, respectively, and their contributions are shared according to load profile, since the modulation is mainly performed by CHP1 during off-peak load, whereas CHP2 is run almost close to nominal value in the second half of the day. Whereas 2.8% of daily electric load is satisfied by ESS and 7.4% by electricity exchange at PCC. The total MG demand is 3.8% higher than load, due to ESS charging. Moreover, 0.8% of internal production is sold to the grid in central hours of the day (i.e. when renewables exceed the remaining 20% of load), and this is reported in Fig. 6 as the difference between the envelope of bars and the dashed red curve.

Thermal power balance is illustrated in Fig. 7. In this case, thermal load is mainly satisfied by CHP systems, and an excess thermal power is registered (roughly 5.9% of the total daily amount), especially in the morning and in the presence of peak electric load, as a by-product of electric load tracking. B2 is off over the whole day and B1 contributes only by 1.4% to load coverage in peak intervals, when the contemporaneous extra-production by RES does not allow CHPs to produce more thermal power.

Published source: http://dx.doi.org/10.1016/j.segan.2017.07.003

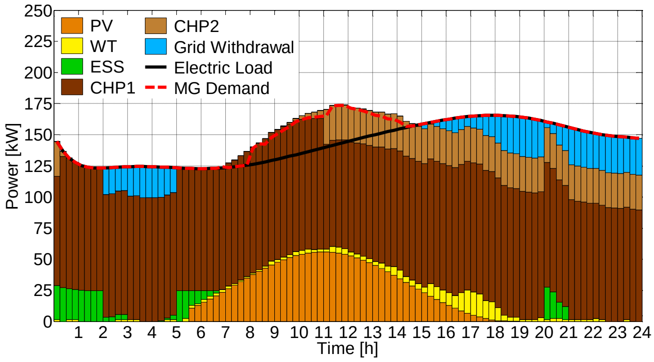

Fig. 6. C1 Strategy: electrical power balance.

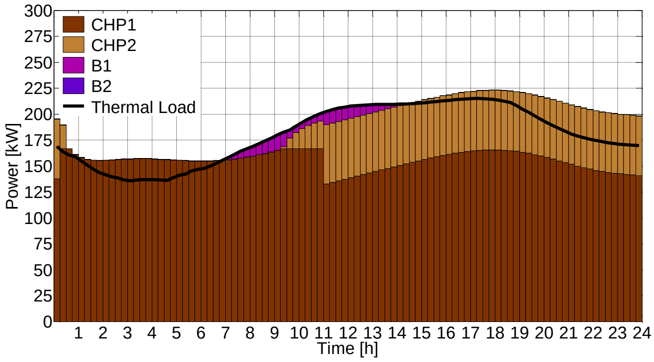

Fig. 7. C1 Strategy: thermal power balance.

4.2.3. Thermal Load Tracking – C2 Strategy

The C2 strategy described in Section 3.2 is implemented by adding eq. (26) to the set of equality constraints and setting the coefficient $\alpha_{ht} = 0.8$ for the whole day. Both CHP systems are involved in the strategy, i.e. $u_{it}^{M} = 1$ and $u_{kt}^{R} = 1 \ \forall t$.

The relevant electric power sharing is illustrated in Fig. 8. It can be noted that 61.6% of electric load is matched by CHP systems, 25.0% by electricity exchange at PCC and the contribution of ESS is less intense, at 2.7%. The total MG demand is 3.7% higher than load profile, corresponding to ESS charge, and no grid injection is observed.

Thermal power balance is reported in Fig. 9. It can be observed that CHP units share the prescribed amount of thermal load according to economic merit. Indeed, CHP1 is

Published source: http://dx.doi.org/10.1016/j.segan.2017.07.003

working throughout the day and covers 70.3% of thermal demand, and CHP2 is exploited only in periods with higher demand, satisfying 9.7%. Furthermore, B1 runs close to its rated power covering 10.5% of thermal demand, whereas more expensive B2 has a daily demand share of 11.0%, most concentrated in peak demand hours.

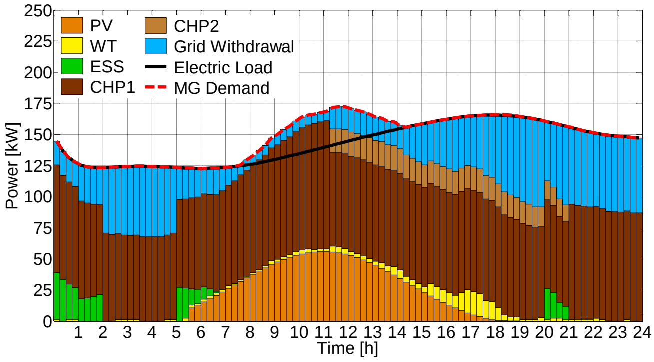

Fig. 8. C2 Strategy: electrical power balance.

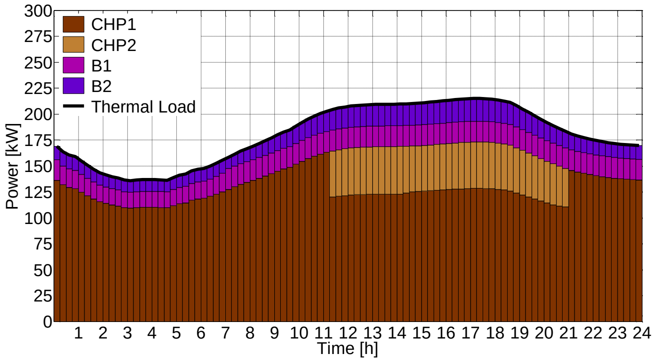

Fig. 9. C2 Strategy: thermal power balance.

4.2.4. On-Off Operation – C3 Strategy

The C3 strategy is considered by including eq. (27.a)-(27.b) in problem formulation. This simulation set is aimed at investigating the time intervals when the strategy yields the most efficient MG operating condition. This preliminary investigation yielded the activation of C3 strategy in the period from hour 11 to hour 19 for CHP1 ($\beta_{kt}^{R} = 1 \ \forall \, t \in [45, 76]$), whereas for CHP2 it is not considered.

Published source: http://dx.doi.org/10.1016/j.segan.2017.07.003

The electric power balance is depicted in Fig. 10. Due to strategy implementation, CHP systems cover 76.0% of load. An amount of exchange power at PCC corresponding to 11.2% of load is observed and ESS contribute to 2.8%. Total MG generation exceeds the imposed load by 4.4%. The production surplus at strategy activation yields an excess production amounting to 0.6% of the load, that is sold to the distribution network. Indeed, the remaining 3.8% is dedicated to ESS charge.

Thermal power balance in Fig. 11 shows that CHP systems are entrusted to cover 98.1% of thermal demand (CHP1 covers 86.7% and CHP2 11.4%), whereas boilers are called to satisfy the residual demand until hour 11, and in the peak hours they are unexploited. A slight excess of thermal power production is observed in the period of strategy activation.

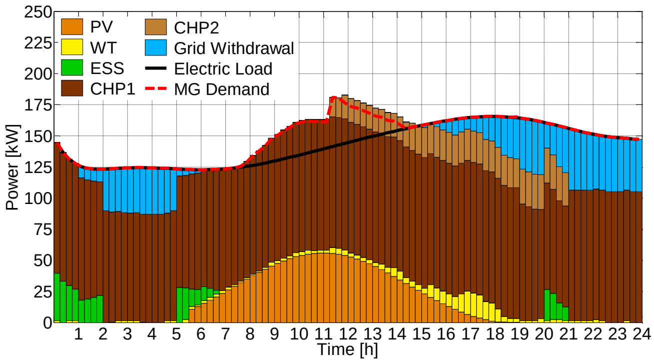

Fig. 10. C3 Strategy: electrical power balance.

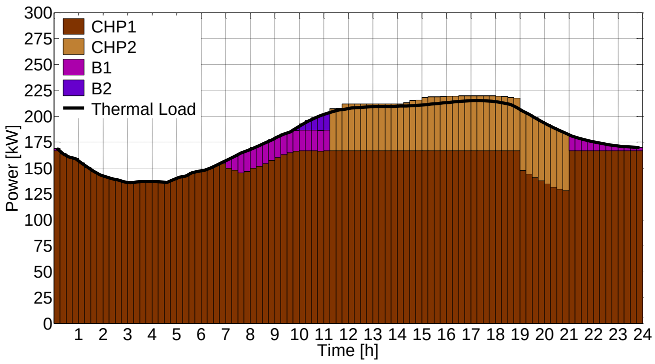

Published source: http://dx.doi.org/10.1016/j.segan.2017.07.003

Fig. 11. C3 Strategy: thermal power balance.

4.3. Strategy Comparison and Discussion

Technical and economic issues of the implemented strategies in the day-ahead operation planning of the MG can be compared. In particular, in Table 3 the total daily cost of each strategy is reported, and the contribution of main cost items is detailed.

Table 3. Daily cost and contributions

Strategies / Costs	Base Case	C1	C2	C3
Electricity purchase	€ 52.87	€ 33.66	€ 114.16	€ 51.20
CHP fuel cost	€ 440.87	€ 477.17	€ 367.77	€ 448.22
Boiler fuel cost	€ 8.19	€ 3.25	€ 51.96	€ 6.53
Energy selling revenue	€ 0.00	– € 1.61	€ 0.00	– € 1.28
Emission cost	€ 4.69	€ 4.99	€ 3.90	€ 4.74
TOTAL COST	**€ 506.62**	**€ 517.46**	**€ 537.79**	**€ 509.41**

It can be observed C2 strategy reveals the most expensive, with a maximum difference of 6% with respect to the Base Case.

One of the main factors yielding differences in daily cost is the amount of electricity exchange at PCC with the distribution network, whose trends, determined as $P_{Pt} - P_{Dt}$, are shown in Fig. 12. In fact, the highest positive values, i.e. power withdrawal P_{Pt}, are reached in C2 strategy and the lowest values are observed in C1 strategy. It can be pointed out that, in all cases, the electricity withdrawal is reduced when electricity cost is higher (hours 20-21). Power delivery P_{Dt} is observed in cases C1 and C3 in central hours of the day, when the excess comes for free from renewables due to the application of specific strategy. Whereas, fuel cost is higher in Case C1 due to the more intense exploitation of the CHP systems.

Published source: http://dx.doi.org/10.1016/j.segan.2017.07.003

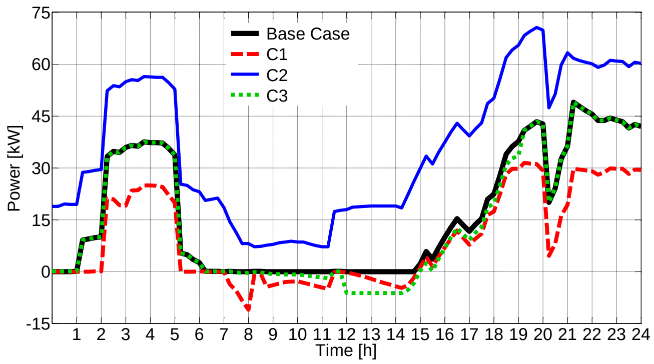

Fig. 12. Electricity exchange at PCC with the distribution network in the strategies.

SOC trends for ESS, in p.u. of total capacity, are illustrated in Fig. 13. It can be noted that SOC at the end of the day returns to initial value, according to the constraint (3.b). This behavior contributes to extend ESS life as well, since it depends on the number of charge/discharge cycles [27].

ESS has the task of storing excess energy, especially in hours 9-13 when RES production is high and the electricity price is generally low. This yields an increase of total MG demand, and limits power injection into the network. In fact, storing energy in excess production periods and using it, even considering non-ideal efficiencies, to cover the demand in peak price periods (hours 20-21), reveals in general more convenient than selling excess production and buying energy in peak price hours. Moreover, the ESS is discharged until hour 6, covering part of the load demand and avoiding network withdrawal, in order to be ready to charge in the presence of excess power. Correspondently, minimum SOC of 30 kWh (0.21 p.u.) is observed in C3, along with maximum daily energy of 94.4 kWh. Slight differences are observed with respect to Base Case in C1, with deeper discharge in hour 3. Minimum exploitation of ESS is observed in C2 with daily energy supply of 91.5 kWh, and those differences are highlighted in the details at bottom of Fig. 13.

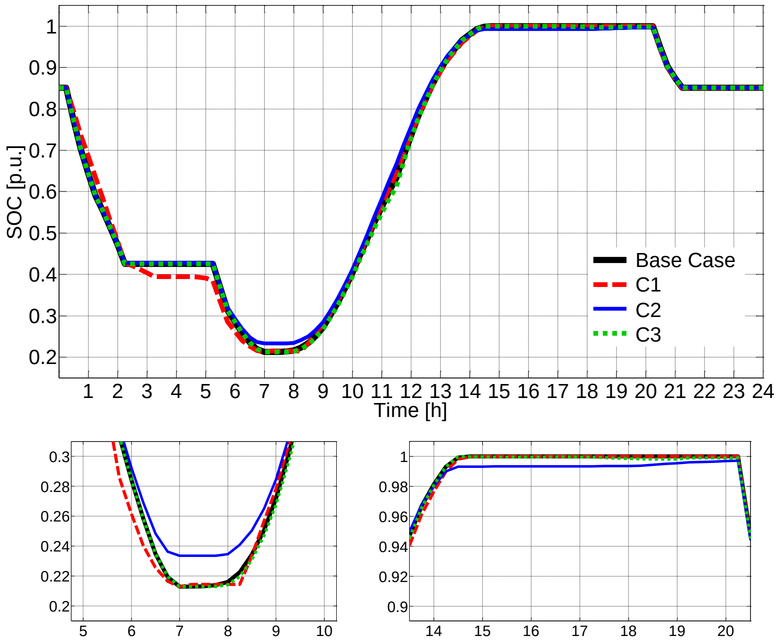

Fig. 13. SOC of ESS in the strategies.

It can be observed that in Base Case and C2 the thermal demand is strictly satisfied during the day, i.e. constraint (24) reduces to an equality, whereas the excess thermal power is due only to CHP strategies. Being less efficient, boilers are usually called to compensate for peak load, and B2 reveals the less preferable. In addition, in C1 and C3 Strategies the CHP systems reach a global average efficiency, given by the sum of electrical and thermal efficiencies, higher than 75%. This threshold often characterizes cogeneration systems with high-efficiency.

As regards emissions, their contribution range from 0.75% to 1.0% of total daily cost. In particular, C1 strategy shows higher emissions (1,241 kg of CO_2 in a day), whereas C2 reveals the less pollutant one (971 kg of CO_2 in a day). However, it can be seen that higher emissions are not related to higher total cost.

In CHP operation programs resulting from the procedure, it is observed that production level does not fall below experimental minimum amount (1 kW), since the corresponding low efficiency, and consequent high cost, makes it inconvenient to use CHP below 1 kW with respect to other sources. This allows to achieve analogous results with respect to other approaches introducing integer decision variables [24][64].

In order to validate the optimality of the achieved solution, obtained by the NLP formulation solved through SQP starting from the solution of the linearized problem, a set of further 100 starting points satisfying the constraints of the linearized problem is exploited [65]. These starting points are generated by stochastic variations of the linearized problem solution, according to normal distributions with zero mean and 20% as confidence interval for each state variable. The problem is therefore solved through SQP by using each of these starting points, and the obtained results for the Base Case are reported in Fig. 14, where their cumulative distribution is compared with the solution of the proposed method. It can be seen that the solution obtained by means of the method described in Section 4.1 is the lowest, and most of solutions with stochastic starting points are close, but not better. Analogous results are obtained for the other three cases. Therefore, these results confirm that the overall proposed procedure for NLP problem solution, where the starting point is the solution of the linearized problem, reasonably guarantees the achievement of the optimal solution.

Published source: http://dx.doi.org/10.1016/j.segan.2017.07.003

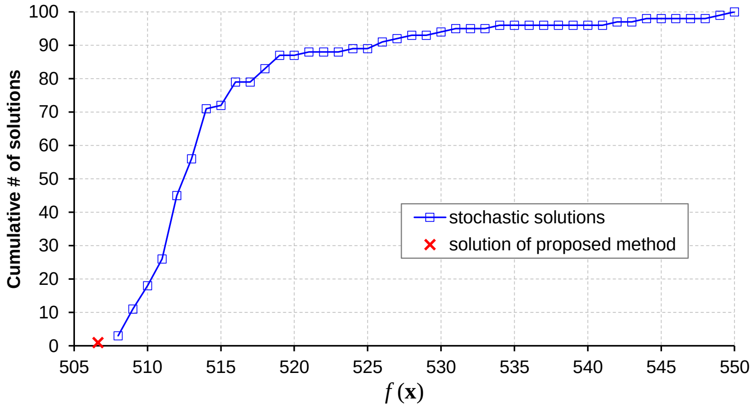

Fig. 14. Comparison of solutions with different starting points in the Base Case.

5. Conclusions

In this paper, an optimization procedure for the day-ahead operational scheduling of a MG has been proposed. A non-linear programming problem is formulated, accounting for actual features of DG technologies and for different energy pricing schemes. Electric and thermal generation systems, along with CHP devices, have been modeled and the operation of ESS has been taken into account, in order to minimize operational costs on a daily horizon while satisfying electric and thermal load. Moreover, different strategies have been exploited according to operating modes of CHP systems. These strategies have been tested by implementing case studies on an experimental MG and comparing technical and economic outcomes. Simulation results have proved that the different strategies remarkably affect operation costs, reaching significant reduction of primary energy consumption and pollutant emissions. Strategy effectiveness depends on MG structure and particular condition of the considered day. The proposed approach is flexible enough to incorporate other types of DG units.

Future work will deal with the inclusion of thermal storage, the simulation of periods with different connection modes (islanded or grid-connected), and the implementation of the second-stage procedure to cope with deviations of renewable production and load from the predicted levels in the real time. Finally, the application in actual SCADA/EMS system for MG management is envisaged, as exemplified in [66] for a different configuration.

References

[1] D. E. Olivares, A. Mehrizi-Sani, A. H. Etemadi, C. A. Canizares, R. Iravani, M. Kazerani, A. H. Hajimiragha, O. Gomis-Bellmunt, M. Saeedifard, R. Palma-Behnke, G. A. Jimenez-Estevez, N. D. Hatziargyriou, "Trends in microgrid control," *IEEE Trans. Smart Grid*, vol. 5, no. 4, pp. 1905–1919, Jul. 2014. http://dx.doi.org/10.1109/TSG.2013.2295514 .

[2] C. Chowdhury, S.P. Chowdhury, P. Crossley, *Microgrids and Active Distribution Networks*. London, UK: IET, 2009. http://dx.doi.org/10.1049/PBRN006E .

[3] C. Natesan, S.K. Ajithan, S. Chozhavendhan, A. Devendhiran, "Power Management Strategies in Microgrid: A Survey", *International Journal of Renewable Energy Research*, Vol. 5 No. 2, pp. 1-7, 2015.

[4] Z. Bao, Q. Zhou, Z. Yang, Q. Yang, L. Xu, T. Wu, "A Multi Time-Scale and Multi Energy-Type Coordinated Microgrid Scheduling Solution—Part I: Model and Methodology", *IEEE Transactions on Power Systems*, vol. 30, No. 5, pp. 2257-2266, Sept. 2015, http://dx.doi.org/10.1109/TPWRS.2014.2367127 .

[5] A. A. Khan, M. Naeem, M. Iqbal, S. Qaisar, A. Anpalagan, "A compendium of optimization objectives, constraints, tools and algorithms for energy management in microgrids", Renewable and Sustainable Energy Reviews vol. 58, pp. 1164-1683, 2016, http://dx.doi.org/10.1016/j.rser.2015.12.259 .

[6] H. Daneshi, H. Khorashadi-Zadeh, "Microgrid Energy Management System: A Study of Reliability and Economic Issues", " in *Proc. IEEE Power Energy Soc. Gen. Meeting*, San Diego, CA, 2012, pp. 1–5. http://dx.doi.org/10.1109/PESGM.2012.6344957 .

[7] J. Chen, X. Yang, L. Zhu, M. Zhang, "Microgrid Economic Operation and Research on Dispatch Strategy", In *Proc. Power Engineering and Automation Conference (PEAM)*, Wuhan, 2012 pp. 1-6. http://dx.doi.org/10.1109/PEAM.2012.6612416 .

[8] G.-C. Liao, "The Optimal Economic Dispatch of Smart Microgrid Including Distributed Generation", In *Proc. IEEE 2nd Int. Symp. on Next-Generation Electronics (ISNE)*, Kaohsiung, 2013, pp. 473-477. http://dx.doi.org/10.1109/ISNE.2013.6512401 .

[9] A. Chaouachi, R.M. Kamel, R. Andoulsi, K. Nagasaka, "Multiobjective Intelligent Energy Management for a Microgrid", *IEEE Trans. Ind. Electron.*, vol. 60, no. 4, pp. 1688–1699, Apr. 2013. http://dx.doi.org/10.1109/TIE.2012.2188873 .

[10] R. Palma-Behnke, C. Benavides, F. Lanas, B. Severino, L. Reyes, J. Llanos, D. Saez, "A Microgrid Energy Management System Based on the Rolling Horizon Strategy", *IEEE Trans. Smart Grid*, vol. 4, no. 2, pp. 996–1006, Jun. 2013. http://dx.doi.org/10.1109/TSG.2012.2231440

[11] Q. Jiang, M. Xue, G. Geng, "Energy Management of Microgrid in Grid-Connected and Stand-Alone Modes", *IEEE Trans. Power Syst.*, vol. 28, no. 3, pp.3380 -3389, Aug. 2013. http://dx.doi.org/10.1109/TPWRS.2013.2244104 .

[12] M. Strrelec, J. Berka, "Microgrid Energy Management based on Approximate Dynamic Programming", *in Proc. 4th IEEE/PES ISGT Europe*, Copenhagen, Denmark, 2013, pp. 1-5. http://dx.doi.org/10.1109/ISGTEurope.2013.6695439 .

[13] M. Mahmoodi, P. Shamsi, B. Fahimi, "Optimal Scheduling of Microgrid Operation Considering the Time-of-Use Price of Electricity", Industrial Electronics Society, IECON 2013, Vienna, 2013, Pages 2127-2132. http://dx.doi.org/10.1109/IECON.2013.6699460 .

[14] D. Zhang, S. Li, P. Zeng, C. Zang, "Optimal Microgrid Control and Power Flow Study With Different Bidding Policies by Using PowerWorld Simulator", *IEEE Trans. Sustain. Energy*, vol. 5, no. 1, pp. 282-292, Oct. 2014. http://dx.doi.org/10.1109/TSTE.2013.2281811

[15] M. Ross, C. Abbey, F. Bouffard, G. Joos, “Multiobjective Optimization Dispatch for Microgrids With a High Penetration of Renewable Generation”, *IEEE Trans. Sustain. Energy*, vol. 6, no. 4, pp. 1306-1314, Oct. 2015. http://dx.doi.org/10.1109/TSTE.2015.2428676 .

[16] V. Prema, K. Uma Rao, “Predictive Models For a Power Management Of a Hybrid Microgrid-A Review”, in *Proc. Int. Conf. Advances in Energy Conversion Technologies (ICAECT)*, Manipal, 2014, pp. 7-12. http://dx.doi.org/10.1109/ICAECT.2014.6757053 .

[17] I. Prodan, E. Zio, “An optimization-based control approach for reliable microgrid energy management under uncertainties”, in *Proc. IEEE ISEPS Workshop*, Bucharest, 2013, pp. 4-7. http://dx.doi.org/10.1109/ISEPS.2013.6707950 .

[18] R. A. Gupta, N. K. Gupta, “A robust optimization based approach for microgrid operation in deregulated environment”, *Energy Conversion and Management*, vol. 93, pp. 131-131, 2015, http://dx.doi.org/10.1016/j.enconman.2015.01.008 .

[19] S. A. Alavi, A. Ahmadian, M. Aliakbar-Golkar, “Optimal probabilistic energy management in a typical micro-grid based-on robust optimization and point estimate method”, *Energy Conversion and Management*, vol. 95, pp. 314-325, 2015, http://dx.doi.org/10.1016/j.enconman.2015.02.042 .

[20] C. Marnay, G. Venkataramanan, G. Stadler, A. Siddiqui, R. Firestone, R. Chandran “Optimal technology selection and operation of microgrids in commercial buildings”, *IEEE Trans Power Syst.* Vol. 23, no. 3, pp. 975-982, 2008, http://dx.doi.org/10.1109/TPWRS.2008.922654 .

[21] M. Motevasel, A. R. Seifi, T. Nikham, “Multi-objective Energy management of CHP (combined heat and power)-based micro-grid”, *Energy*, vol. 51, pp. 123-136, 2013, http://dx.doi.org/10.1016/j.energy.2012.11.035 .

[22] G. Bruni, S. Cordiner, V. Mulone, V. Rocco, F. Spagnolo, “A study on the Energy management in domestic micro-grids based on Model Predictive Control Strategies”, *Energy Conversion and Management*, vol. 102, pp. 50-58, 2015, http://dx.doi.org/10.1016/j.enconman.2015.01.067 .

[23] X. Lin, P. Li, J. Ma, Y. Tian, D. Su, “Dynamic Optimal Dispatch of Combined Heating and Power Microgrid Based on Leapfrog Firefly Algorithm”, Proc. of 2015 IEEE 12th Int. Conf. on Networking, Sensing and Control, Taipei, Taiwan April 9-11, 2015, pp. 416-420.

[24] M. Alipour, B. Mohammadi-Ivatloo, “Stochastic Scheduling of Renewable and CHP-Based Microgrids”, IEEE Trans. Industrial Informatics, vol. 11, no. 5, pp. 1049-1058, October 2015, http://dx.doi.org/10.1109/TII.2015.2462296 .

[25] K. Basu, A. Bhattacharya, S. Chowdhury, S.P. Chowdhury, “Planned Scheduling for Economic Power Sharing in a CHP-Based Micro-Grid”, IEEE Trans. Power Systems, vol. 27, no. 1, pp. 30-38, February 2012, http://dx.doi.org/10.1109/TPWRS.2011.2162754 .

[26] X. Jin, H. Li, T. Jin, X. Xu, M. Wang, J., Meng, “Economical and Coordinated Dispatch of CHP Based Microgrid with Renewable Energy Resources”, Advanced Materials Research Vols. 960-961, pp. 1022-1028, 2014 http://dx.doi.org/10.4028/www.scientific.net/AMR.960-961.1022

[27] L. Majic, I. Krzelj, M. Delimar, “Optimal scheduling of a CHP system with energy storage”, Proc. of MIPRO 2013, May 20-24, 2013, Opatija, Croatia, pp. 1253-1257.

[28] D. Zhang, S. Evangelisti, P. Lettieri, L.G. Papageorgiou, “Economic and environmental scheduling of smart homes with microgrid: DER operation and electrical tasks”, Energy Conversion and Management, vol. 110, pp. 113-124, 2016, http://dx.doi.org/10.1016/j.enconman.2015.11.056

[29] K.C. Kavvadias, A.P. Tosios, Z.B. Maroulis, “Design of a combined heating, cooling and power system: Sizing, operation strategy selection and parametric analysis”, *Energy Convers. and Managem.*, vol. 51, pp. 833-845, 2010, http://dx.doi.org/10.1016/j.enconman.2009.11.019

[30] E. Carpaneto, G. Chicco, P. Mancarella, A. Russo, “Cogeneration planning under uncertainty-Part I: Multiple time frame approach”, *Appl. Energy*, vol. 88, no. 4, pp. 1075-1083, 2011. http://dx.doi.org/10.1016/j.apenergy.2010.10.014 .

[31] E. Perea, N. Ruiz, I. Cobelo, Z. Lizuain, A. Carrascal, "A novel optimization algorithm for efficient economic dispatch of Combined Heat and Power devices", *Energy and Buildings*, vol. 111, pp. 207-514, January 2016. http://dx.doi.org/10.1016/j.enbuild.2015.11.025

[32]H. Bowen. Z. Zhanghua, "Stochastic Multi-objective Dynamic Optimal Dispatch for Combined Heat and Power Microgrid", *Proc. of 2016 IEEE PES Asia-Pacific Power and Energy Conference (APPEEC)* – Xi'an, China, 25-28 October 2016, pp. 2369-2373, http://dx.doi.org/10.1109/APPEEC.2016.7779908

[33] M. Barbarić, D. Lončar, "Energy management strategies for combined heat and electric power micro-grid", *Thermal Science*, vol. 20, no. 4, pp. 1091-1103, 2016. http://dx.doi.org/10.2298/TSCI151215081B .

[34] L. Ma, N. Liu, J. Zhang, W. Tushar, C. Yuen, "Energy Management for Joint Operation of CHP and PV Prosumers Inside a Grid-Connected Microgrid: A Game Theoretic Approach", *IEEE Trans. Industrial Informatics*, vol. 12, no. 5, pp. 1930-1942, October 2016. http://dx.doi.org/10.1109/TII.2016.2578184 .

[35] T. Schittekatte, M. Stadler, G. Cardoso, S. Mashayekh, N. Sankar, "The impact of short-term stochastic variability in solar irradiance on optimal microgrid design", *IEEE Transactions on Smart Grid*, accepted 2016 http://dx.doi.org/10.1109/TSG.2016.2596709 .

[36] M.J. Sanjari, H. Karami, H.B. Gooi, "Micro-generation dispatch in a smart residential multi-carrier energy system considering demand forecast error", *Energy Conv. and Manag.* vol. 120, pp. 90-99, July 2016. http://dx.doi.org/10.1016/j.enconman.2016.04.092 .

[37] J. Aghaei, M.-I. Alizadeh, "Multi-objective self-scheduling of CHP (Combined heat and power)-based microgrids considering demand response programs and ESSs (energy storage systems)", *Energy*, vol. 55, pp. 1044-1054, June 2013. http://dx.doi.org/10.1016/j.energy.2013.04.048 .

[38] M. Restepo, C. A. Canizares, M. Kazerani, "Three-Stage Distribution Feeder Control Considering Four-Quadrant EV Chargers", *IEEE Transactions on Smart Grid*, Accepted December 2016, http://dx.doi.org/10.1109/TSG.2016.2640202 .

[39] S. S. Soman, H. Zareipour, O. Malik, P. Mandal, "A review of wind power and speed forecasting methods with different time horizons", in *Proc. North Amer. Power Symp*. (NAPS), Arlington, 2010, pp.1-8. http://dx.doi.org/10.1109/NAPS.2010.5619586 .

[40] J. A. Duffie, W. A. Beckman, *Solar Engineering of Thermal Processes*. Fourth Edition , John Wiley & Sons, Inc., Hoboken, NJ, USA.2013.. http://dx.doi.org/10.1002/9781118671603

[41] E. Skoplaki, A.G. Boudouvis, J.A. Palyvos, "A simple correlation for the operating temperature of photovoltaic modules of arbitrary mounting", *Solar Energy Mater. Solar Cells*, vol. 92, no. 11, pp.1393-1402, 2008. http://dx.doi.org/10.1016/j.solmat.2008.05.016 .

[42] J. Shi, W.-J. Lee, Y. Liu, Y. Yang, P. Wang, "Forecasting Power Output of Photovoltaic Systems Based on Weather Classification and Support Vector Machines", *IEEE Trans. Ind. Appl.*, vol. 48, no. 3, pp. 1064-1069, May/June 2012: http://dx.doi.org/10.1109/TIA.2012.2190816 .

[43] O. H. Mohammed, Y. Amirat, M. Benbouzid, T. Tang, "Hybrid Generation Systems Planning Expansion Forecast: A critical State of the art review", *Proc. of 39th IECON IEEE IES Annual Conference*, Vienna, 2013, pp. 1668-1673: http://dx.doi.org/10.1109/IECON.2013.6699383 .

[44] L. H. Macedo, J. F. Franco, M. J. Rider, R. Romero, "Optimal Operation of Distribution Networks Considering Energy Storage Devices", *IEEE Trans. Smart Grid*, vol. 6 no. 6, Nov. 2015, pp. 2825-2836: http://dx.doi.org/10.1109/TSG.2015.2419134 .

[45] B. Zhao, X. Zhang, J. Chan, C. Wang, L. Guo, "Operation Optimization of Standalone Microgrids Considering Lifetime Characteristics of Battery Energy Storage System", *IEEE Trans. Sust. Energy*, vol. 4, no., 4, pp. 934-943, October 2013. http://dx.doi.org/10.1109/TSTE.2013.2248400

[46] M. Gitizadeh, H. Fakharzadegan, "Battery capacity determination with respect to optimized energy dispatch schedule in grid-connected photocvoltaic (PV) systems", *Energy*, vol. 65, pp. 665-674, February 2014. http://dx.doi.org/10.106/j.energy.2013.12.018

[47] E. Hittinger, T. Wiley, J. Kluza, J. Whitacre, “Evaluating the value of batteries in microgrid electricity systems using an improved Energy Systems Model”, *Energy Conv. and Manag.*, vol. 89, pp. 458-472, January 2015. http://dx.doi.org/10.1016/j.enconman.2014.10.011

[48] A.F. Orlando, M.M. Huamaní, L. DoVala, J.V. Araujo, “A methodology for evaluating field performance and emissions of a gas microturbine based cogeneration system”, *Engenharia Térmica*, vol. 7, n. 1, pp.21-30, 2008.

[49] H. Kanchev, F. Colas, V. Lazarov, B. Francois, “Emission reduction and economical optimization of an urban microgrid operation including dispatched PV-based active generators”, *IEEE Transactions On Sustainable Energy*, vol. 5, no. 4, pp. 1397-1405, Oct. 2014. http://dx.doi.org/10.1109/TSTE.2014.2331712 .

[50] A. Rosato, S. Sibilio, “Calibration and validation of a model for simulating thermal and electric performance of an internal combustion engine-based micro-cogeneration device”, *Applied Thermal Engineering*, vol. 45-46, pp. 79-98, Dec. 2012. http://dx.doi.org/10.1016/j.applthermaleng.2012.04.020

[51] N. Badea, *Design for Micro-Combined Cooling, Heating and Power Systems*. London: Springer, 2015. http://dx.doi.org/10.1007/978-1-4471-6254-4

[52] Deliberazione AEEG 493/2012/R/efr “Approvazione delle modalità per l’attribuzione dei corrispettivi di sbilanciamento e dei corrispettivi a copertura dei costi amministrativi da attribuire ai produttori in regime di ritiro dedicato e di tariffa fissa onnicomprensiva”, 22 November 2012 (in Italian).

[53] A. Cagnano, E. De Tuglie, M. Dicorato, G. Forte, M. Trovato, “PrInCE Lab experimental microgrid – Planning and operation issues”, *Proc. of 2015 IEEE 15th EEEIC Int. Conf.*, Rome, Italy, pp. 1671-1676, http://dx.doi.org/10.1109/EEEIC.2015.7165423 .

[54] B. Aluisio, A. Cagnano, E. De Tuglie, M. Dicorato, G. Forte, M. Trovato, “An architecture for the monitoring of microgrid operation”, *Proc. of 2016 IEEE EESMS Conference*, Bari, Italy, pp. 1-6, http://dx.doi.org/10.1109/EESMS.2016.7504809 .

[55] http://www.wunderground.com/

[56] http://www.amgasbarisrl.it/ (in Italian)

[57] http://www.sendeco2.com .

[58] A. Bhatt, A. Shrivastava, M. Pandit, H. M. Dubey, "Dynamic Scheduling of Operating Energy and Reserve in Electricity Market with Ramp Rate Constraints", *in Proc. IEEE IET CRAIE-2014 Conf.*, Jaipur, India, May 2014, pp. 1-6. http://dx.doi.org/10.1109/ICRAIE.2014.6909313

[59] F. A. Bayer, G. Notarstefano, F. Allgower, "A Projected SQP method for Nonlinear Optimal Control with Quadratic Convergence", Proc. of 52nd IEEE Conference on Decision and Control, December 10-13, 2013, Florence, Italy, pp. 6463-6468, http://dx.doi.org/10.1109/CDC.2013.6760912

[60] P. E. Gill., E. Wong, "Sequential quadratic programming methods", in: J. Lee, S. Leyffer, "Mixed Integer Nonlinear Programming", Vol. 147 of The IMA Volumes in Mathematics its Applications, Springer Science, 2012, pp. 147-224, http://dx.doi.org/10.1007/978-1-4614-1927-3_6

[61] J. Nocedal, S. J. Wright, "Numerical Optimization – Second Edition". Springer Series in Operations Research, Springer Verlag, 2006.

[62] A. D. Belegundu, T. R. Chandrupatla, "Optimization Concepts and Applications in Engineering – Second Edition", Cambridge University Press, 2011.

[63] D. P. Bertsekas, "Nonlinear Programming: 3rd Edition", Athena Scientific, 2016.

[64] I. G. Moghaddam, M. Saniei, E. Mashhour, "A comprehensive model for self-scheduling an energy hub to supply cooling, heating and electrical demands of a building", *Energy*, vol. 94, pp. 157-170, January 2016. http://dx.doi.org/10.1016/j.energy.2015.10.137

[65] R. Fourer, D. M. Gay, B. W. Kernighan, "AMPL: A Modeling Language for Mathematical Programming – Second Edition", Duxbury Press / Brooks / Cole Publishing Company, 2003.

[66] B. Aluisio, A. Cagnano, E. De Tuglie, M. Dicorato, G. Forte, M. Trovato, "PrInCE lab microgrid: Early experimental results", *2016 AEIT International Annual Conference (AEIT)*, Capri (Italy), 5-7 Oct. 2016, pp. 1-6, http://dx.doi.org/10.23919/AEIT.2016.7892770